Space and Time Resolved Electron Density and Current Measurements in a Dense Plasma Focus Z-Pinch

Niansheng Qi, *Member, IEEE*, Steven F. Fulghum,
Rahul R. Prasad, *Member, IEEE*, and Mahadevan Krishnan, *Member, IEEE*

***Abstract*—Plasma density and current profiles in a Z-pinch are important parameters to understand the implosion and radiation physics. This paper describes measurements of electron density and current at radii of $\geq 200\mu$m from the axis of a dense plasma focus (DPF) pinch plasma that is imploded by a $\approx$0.3 MA current pulse. These measurements use laser interferometry and polarimetry. The electromagnetic wave propagating through a current carrying plasma will change its phase, polarization state, and propagation direction. Refraction by electrons bends the wave fronts and changes the propagation direction; Faraday rotation due to the magnetic field and electron density rotates the laser polarization vector. By measuring these quantities simultaneously, the magnetic field and electron density can be separately determined. Although the DPF used here is a low current device, the measured densities ($\leq 10^{20}$ cm^{-3}) and magnetic fields ($\sim$100 T) are similar to values expected just outside higher current but larger radius Z-pinches, so this technique should be applicable there as well. The techniques described here do not require access to the core of the pinch to work; just outside these pinches the coronal density and self magnetic field are high enough to give reliable data but not so high as to make the measurements difficult.**

***Index Terms*—Dense plasma focus, Faraday rotation, plasma refraction, shearing interferometry, Z-pinch plasma.**

I. Introduction

UNDERSTANDING the implosion dynamics and stagnation physics of Z-pinches requires time and space resolved measurements of the current and plasma density. Presently, the implosion current in high current drivers is measured by using Rogowski coils, resistive shunts, and/or B-dot current sensors. It is typically measured only beyond $r \geq 30$ mm, outside the entire radial excursion of the pinch plasmas. In most high current pinches the current has been measured only at radii >20 times the final pinch radius. The technique described here gives data within 1–3 times the pinch radius, but not inside the core. Available instruments tend to focus on the X-ray emission after the pinch has already assembled on axis. But the efficiency with which the pinch converts the available reservoir of streaming kinetic and magnetic energy into X-rays is determined by the detailed history of the density, temperature, plasma resistivity, and current flow in the pinch during the radial motion, as well as by the end state of the pinch. Better measurements are needed of the motion of the plasma shell and current sheath from their initial states to their final states. Such information can be obtained from temporally and spatially resolved plasma density and current measurements.

To measure the electron density in plasmas, laser interferometry in a Mach–Zehnder configuration is commonly used. Mach–Zehnder interferometers are capable of measuring fringe shifts from 10^{-4} to a few waves, but they may not be suitable for high current implosion pinch plasmas since the fringe shifts produced are too large. The magnetic field in plasmas is typically measured by magnetic probes, spectroscopic methods based on the Zeeman effect and Faraday rotation methods. The magnetic probe is simple but has poor spatial resolution and is not suitable for high current pinches, which are severely perturbed by invasive probes. In dense Z-pinch plasmas the Zeeman shift is swamped by much larger Doppler and Stark line widths. Also, in a dense pinch plasma the continuum radiation can be so strong that visible and/or ultraviolet (UV) line radiation profiles are often not detectable above this background.

Polarimeter-interferometer systems have been used in the past for electron density and magnetic field measurements in high current Z-pinches. Faraday rotation images and interferograms from a $\sim$1 MA dense plasma focus (DPF) plasma have been obtained, in which the electron densities were deduced from Mach–Zehnder interferograms and the Faraday rotation angles from the differential intensities on the polarized laser images [1]. However, it is difficult to apply Mach–Zehnder interferometry to higher current pinch plasmas due to the large phase shifts and laser beam refraction out of the optical line of sight. Two-dimensional (2-D) maps of the Faraday rotation angle could be produced in theory, but reading absolute intensity from the images is very difficult, particularly in the presence of background light from the Z-pinch plasma itself.

This paper presents a new approach for electron density and current measurements in and just outside pinch plasmas. Though the experiments were conducted on a $\approx$0.3 MA, 1.7 μs DPF driver, the method can be adapted for higher current Z-pinches with some modifications. The measurements used were based on laser refraction [2], polarimetry [3], [4], and

Manuscript received November 14, 1997; revised April 10, 1998. This work was supported by the Defense Special Weapons Agency (DSWA) via a SBIR Phase I contract.

N. Qi, R. R. Prasad, and M. Krishnan are with Alameda Applied Sciences Corp., San Leandro, CA 94577 USA (e-mail: qi@aasc.net).

S. F. Fulghum is with the Science Research Laboratory, Somerville, MA 02143 USA.

Publisher Item Identifier S 0093-3813(98)06373-5.

lateral shearing interferometry [5], [6]. The electromagnetic wave (of the laser) propagating through a current carrying plasma will change its phase, polarization state, and propagation direction. Refraction by electrons bends the wave fronts and changes the propagation direction; Faraday rotation due to the magnetic field and electron density rotates the polarization vector. By measuring the laser beam refraction angle and polarization states simultaneously in and just outside a Z-pinch plasma, the magnetic field and electron density were separately determined. Furthermore, using the laser shearing image technique to measure larger phase shifts due to the pinch current heath, it was possible to derive the electron density profiles of the pinch.

The advantages of the laser based measurements reported here are that the evolution of the electron density can be followed with high time resolution and that no absolute calibration of the instrumentation is required. With a multichannel interferometry and polarimetry system, electron density and current profiles in dense Z-pinches can be obtained with spatial resolution of $\leq$1 mm. Such measurements can help resolve the uncertainties that remain regarding the form of the electrical resistivity of the plasma, the zone of current conduction, and the electron density distribution. They could also lead to a more comprehensive model that agrees broadly with experiments and leads to better predictive capability for high current accelerators.

The rest of this paper is organized as follows. Section II reviews the principle behind the technique. Section III presents the results of the experiments and data analysis. Conclusions drawn from the experiments and recommendations for future experiments are presented in Section IV.

II. Principle Behind the Technique

A laser beam probe is a noninvasive tool for measuring plasma refractive properties without disturbing the pinch plasma. For typical dense Z-pinch plasmas the phase shift of the probe laser due to the free electron density is $\geq$100 waves. This large level of wavefront distortion can be measured by two techniques.

1) A short pulse, large area probe laser that traverses the entire cross section of the pinch in a shearing interferometer configuration is the best choice for 2-D density profile measurements. A train of short laser pulses provides temporal resolution.
2) A longer pulse (or CW) laser with a narrow waist that traverses just one chord of the pinch diameter. A versatile combination of both a phase shift and a polarization rotation measurement could thus be derived from a single probe beam. After passing through the plasma the single probe would be split into two beams, one for the polarization measurement and one for the phase measurement. This is the best choice for obtaining time-resolved density and current data by measuring the refraction and polarization rotation of the laser due to the plasma refraction and magnetic field. Successive shots along different chords provide spatial resolution (via an Abel inversion).

In the experiments described here, a short pulse (3 ns) laser was used to conduct the laser beam refraction and polarization rotation measurements and to obtain shearing interferograms of the imploding plasma. The principles of these techniques are described below.

A. Refraction and Polarization Rotation of the Laser Beam

When a laser beam of wavelength λ propagates through a current carrying pinch plasma, the refractive index n is, to first order

$$n = \sqrt{1 - \frac{n_e}{n_c}} \cong 1 - \frac{n_e}{2n_c} \tag{1}$$

where n_e is the electron density and n_c (cm^{-3}) $= 1.1 \times 10^{29}\,\lambda^{-2}$ (Å) is the laser cut-off density. The incident polarized laser beam suffers refraction and polarization rotation as it traverses the current carrying pinch plasma. Refraction by electrons bends the beam by an angle θ_r; Faraday rotation due to the magnetic field and electron density rotates the polarization vector by an angle θ_f. As described in [7], these angles are

$$\theta_r = 0.5\,\frac{d}{dy}\int \frac{n_e}{n_c}\,dl \text{ rad} \tag{2}$$

and

$$\theta_r = 2.93 \int \frac{n_e}{n_c}\mathbf{B}\cdot d\mathbf{l} \text{ rad} \tag{3}$$

where y is the shortest distance between the laser and the pinch axis, $\mathbf{B}$ is the self magnetic field due to the current (Tesla) and, $\mathbf{l}$ is the optical path length (cm). Equations (2) and (3) are valid for $\theta_r \ll 1$ and $n_e \ll n_c$, respectively. For simplicity, we assume a cylindrically symmetric (independent of z-direction) Gaussian distribution for the electron density, i.e.,

$$n_e = n_o \exp\left(-\frac{x^2+y^2}{R^2}\right) \tag{4}$$

where R is the plasma mean radius. Assuming that the laser beam travels parallel to the x-axis, the refraction of the laser beam due to the plasma is

$$\theta_r = 0.56\frac{N}{n_c y^2}\left(\frac{y}{R}\right)^3 \exp\left(-\frac{y^2}{R^2}\right) \text{ rad.} \tag{5}$$

where N $(=\pi R^2 n_o)$ is the electron line density. If most of the current flows inside a radius of $r \leq y$, the Faraday rotation angle is,

$$\theta_f = 58.6I\ (\text{MA})\ \frac{N}{n_c y^2}\left(\frac{y}{R}\right)^2 \text{erfc}(y/R) \text{ rad} \tag{6}$$

where I is the implosion current and erfc is the error function. In the experiments, y was fixed. The pinch radius R changes as it implodes on to the axis. Equations (5) and (6) show that

TABLE I
ESTIMATES OF REFRACTION AND FARADAY ROTATION ANGLES FOR Z-PINCH PLASMAS IMPLODED BY 0.3–20 MA CURRENTS

	I(MA)	N(cm^{-1})	R(cm)	y(cm)	θ_r(rad.)	θ_f(rad.)
DPF	0.3	10^{17}	0.025	0.025	0.1	~0.01
Double Eagle	3.5	5×10^{19}	0.15	0.2	0.8	~0.1
Saturn	9	1×10^{20}	0.2	0.4	1	~0.1
Z	20	3×10^{20}	0.3	0.6	2	~0.1

θ_r and θ_f are a function of y/R and have maximum values proportional to N/y^2.

Table I shows some representative values for the electron line density, the pinch plasma radius, the desirable measurement position, and the expected refraction and Faraday rotation angles in Z-pinches imploded by 0.3 to 20 MA drivers, where the electron line density is estimated using the Bennett pinch condition [8]. It is also assumed that most of the implosion current flows within $r \leq y$ and the wavelength of the probe laser is 5000 Å. For a 0.3 MA DPF Z-pinch, it is observed that the refraction and Faraday rotation angles are 0.01-rad, which corresponds to a phase shift of the incident laser of $\approx$100 waves. At higher implosion current levels ($\geq$3 MA), the refraction and Faraday rotation angles are measurable only early in the implosion phase i.e., only at larger radial positions when the current is lower. When the pinch stagnates, the Faraday rotation and/or refraction angles will be too large to measure and too hard to interpret since (5) and (6) are no longer valid. But there is a strong density variation near the edge of the pinch plasma. A corona of lower density might exist outside the pinch. The electron density and the magnetic field in this outer corona are relatively lower than in the pinch core. As a result, the beam refraction and polarization angles in this corona can be measured at a radius not too much greater than that of the pinch plasma and the pinch plasma current is therefore measured just outside the pinch. Large refraction angles not only make the data analysis complicated but it is also difficult to capture the strongly bent beam. A 0.1 rad refraction angle is a reasonable upper bound for the measurements so that the diameter of a collection lens needs to be 5 cm when placed $\approx$20 cm away from the pinch. Using this upper bound for the refraction angle and assuming a Gaussian density profile for the pinch plasmas, the closest radial position of the measurement is estimated using (5) and the corresponding Faraday rotation angles are calculated for different high current pinch drivers, as listed in Table I.

B. A Lateral Shearing Interferometer for 2-D Electron Density Measurements

Lateral shearing interferometry is a widely-used technique for the measurement of wavefront distortions in optical beams [5], [6]. The beam being measured is "self-referenced" by splitting the beam into two parts (after it has been distorted by the refractive medium) and displacing one of the parts laterally by a small amount. Interference is then obtained between the displaced wave fronts and the undisplaced wave fronts. The laser shearing interferometer differs from the Mach–Zehnder interferometer and the Schlieren technique. The Mach–Zehnder interferometer is used to measure the absolute optical phase shift and it is not suitable where there are $\gg$1 wave fringe shifts. The Schlieren technique is suitable for large phase shifts by measuring the first order refraction derivatives due to gradients [9], [10]. But the angular deviations are recorded as intensity variations so that the sensitivity is limited by the dynamic range of the detectors as compared to counting the number of fringes in the shearing images.

Let the wavefront of the distorted probe beam (after passing through the Z-pinch) be described as $W(x, y)$, where x and y are the coordinates of some point P in the transverse plane of the undisplaced part of the probe beam. When the displaced portion wavefront is sheared (moved) in the direction of x by an amount S, then the displaced wavefront error at the same point P is given by $W(x - S, y)$. The resulting path difference δW between the two wavefronts is then given by $W(x, y) - W(x - S, y)$ and interference fringes occur when $\delta W = n\lambda$. A shearing interferogram thus marks out where the difference between the two wavefronts over a shear distance is equal to an integral number of waves. Note that if the shear S is equal to zero then there is no difference between the two wavefronts and there are no fringes regardless of the level of the wavefront distortion. This is the property which makes shearing interferometry so useful for highly distorted wavefronts. When S is very small, the condition for a fringe can be written as

$$\frac{\partial W}{\partial x} \cdot S = n\lambda. \tag{7}$$

Thus the information from the lateral shearing interferometer as we will use it is the ray tilt $\frac{\partial W}{\partial x}$ over the illuminated aperture. With a displacement S, a fringe pattern is produced. Additional phase shifts due to a plasma distort the fringe pattern which gives the density measurement. It should be noted that for a wavefront with spherical curvature, $W = a(x^2 + y^2)$ and the derivative with respect to x gives a set of uniformly spaced fringes parallel to y. Section III shows such a measured fringe pattern from the spherical curved DPF implosion. It is also of interest to note that, in general, shears in both x and y are required to determine a wavefront. In this paper, we have assumed an axisymmetric profile for the electron density, hence we have needed only one shear. Finally, it should also be pointed out that this technique gives a quantitative measure of the density only when the plasma is small compared to the size of the probe beam. Then the interference pattern produced by that portion of the beam that does not interact with the plasma provides the reference level from which the absolute electron density may be determined. Examples of this technique are given in Section III. When the distorting medium is comparable in size to the probe beam, this technique gives only relative densities, like the other techniques. The sensitivity of the measurements is adjustable by choosing proper values for the displacement S.

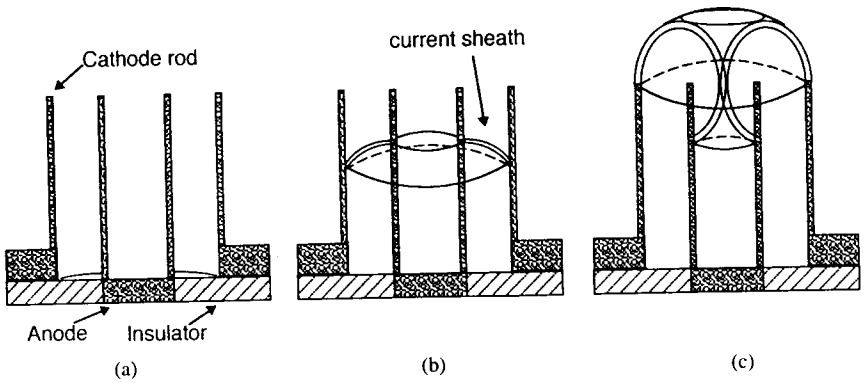

Fig. 1. Schematic drawing of the implosion physics of a DPF. (a) After initiation of the discharge, the quartz insulator breaks down and a current sheath is formed at the insulator surface, (b) the current sheath is accelerated along the coaxial electrodes on a ≈ 1 μs time scale, and (c) radial compression of the plasma on a ≈ 0.2 μs time scale occurs after the current sheath reaches the axial end of the cathode. Intense x-radiation is emitted from the pinched plasma on axis on a $\approx$ 10 ns time scale.

III. Experiments and Results

A 0.3 MA DPF device was used [11] in the experiments. The DPF was driven by a ≈ 54 μF, ≈ 12 nH capacitor bank that was discharged into a gas-filled (vacuum) chamber housing a cylindrical electrode geometry. The bank was charged to ≈ 9 kV with ≈ 2 torr neon gas fill pressure. Under these conditions the peak current was about 0.3 MA and the input energy was 2 kJ. The cylindrical hollow anode of the DPF was 9.5 cm long and 3.4 cm in outer diameter. The cathode consisted of 32 (0.3 cm diameter) rods equally spaced on a 8.2 cm diameter circle.

Fig. 1 shows the implosion physics of a DPF plasma [12]. The energy stored in a capacitor bank is discharged into coaxial, cylindrical electrodes, at a pressure of a few torr of the working gas, e.g., neon. The plasma focus discharge is initiated at the base of the coaxial electrode assembly, where a current-carrying sheath is formed along the quartz insulator. The current sheath, pushed forward by the rising magnetic pressure, quickly separates from the insulator (lift-off phase) and accelerates axially along the two cylindrical electrodes (run-down phase). As the current sheath reaches the end of the electrodes, it turns and moves radially inward (implosion phase) and eventually terminates in the pinch plasma (compression/pinch phase). The compression proceeds until a minimum radius is reached. Intense neon K-shell radiation in a pulse width of ≈ 10 ns is emitted from the pinch plasma column with dimensions of ≈ 0.25 mm radius and ≈ 10 mm length.

A nitrogen laser pumped dye laser was used as the probe beam for the refraction and polarization measurements. The output of the laser was about 10 μJ with pulse duration of ≈ 3 ns at a wavelength of 6000 Å. With a 100 Å narrow band optical filter, the brightness of the laser beam was found to be higher than that of the (continuum) self emission of the pinch plasma by a factor of $\sim 10^4$ when the probe beam was focused down to ~ 50 μm diameter. Often when laser probes are suggested as diagnostics for dense, high current Z-pinches, the question of whether the probe will be swamped by plasma self emission is raised. It is to be noted that in this DPF plasma, we used a 10 μJ laser and found it to be 10^4 times brighter than the plasma, by comparing film negative densities with and without high attenuation filters. A 10–100 mJ laser would be much brighter (in a narrow wavelength band) than Z-pinches from even 3–20 MA drivers. Spatial filters could provide additional suppression of background continuum by a factor of $\geq 100:1$ if desired. Two different sets of measurements are described below.

1) For the beam refraction and Faraday rotation measurements, a pencil laser beam (≈ 1 mm diameter, focused at the pinch to 50 μm diameter) was used. This pencil beam passed close to the axis of the final pinch, at radii equal to or just slightly larger than that of the pinch. As stated earlier, the density at these locations is lower than in the core of the pinch, but the magnetic field has not decayed to much below its peak value. These positions limit the refraction of the laser beam while still giving strong Faraday rotation signals.
2) For the shearing interferograms, the laser was expanded to a ≈ 20 mm diameter beam, so that it was able to capture shearing images of the plasma current sheath (typically < 1 mm in thickness) as it imploded from large radii on to the axis.

A. Beam Refraction and Faraday Rotation Angle Measurements in Pinch Plasmas

Fig. 2 shows the configuration of the single beam refraction and polarization rotation measurements. The laser beam is polarized by passing it through a polarization beam-splitter cube, which has an extinction ratio of $\geq 1000:1$. The P-polarization component of the beam is used for the measurements and the reflected S-polarization of the beam is monitored by a fast photo detector. This photo detector signal is used to accurately determine the laser power and the relative timing between the laser pulse and the pinch plasma. The P-polarization vector of the probe beam is aligned parallel to the pinch axis, which is perpendicular to the self magnetic field B_θ produced by the implosion current. A lens is used to focus the laser beam onto the pinch plasma with a focal spot of ~ 50 μm. The laser focal spot at the pinch plasma position is imaged by a 10 cm diameter, 25 cm focal length lens, which is located 35 cm away from the pinch. Since the typical 1 mm diameter laser beam is much smaller than the 10 cm aperture of the gathering lens, the large lens serves to capture the pencil beam even

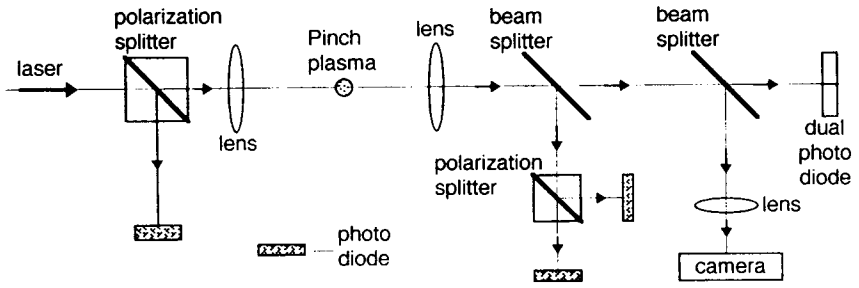

Fig. 2. Experimental arrangement for beam deflection (density) and polarization (magnetic field) measurements.

after strong refraction. After passing through a 100 Å narrow band optical filter, the beam is split and fed into a visible light camera, a polarization analyzer, and a dual photo diode detector. One of the polarized laser beams passes through a polarizing beam-splitter cube oriented at 45° to its original polarization axis. This beam splitter divides the polarization equally between the two photo diodes in the absence of the plasma. Any polarization rotation due to the Faraday effect will direct more of the probe power into one of the photo diodes at the expense of the other. The resulting voltage on the bridge is linearly proportional to the rotation angle for small rotations of up to about ten degrees.

For the refraction angle measurements, a dual photo diode is used which has two rectangular diodes measuring 1.3 × 2.6 mm each, mounted side-by-side to give a 2.6 mm square active area. The laser beam is magnified to ~1 mm in diameter at the dual photo diode. Without the plasma, the two photo cells receive equal amounts of laser power and the output voltage is zero. In the presence of the pinch plasma, the probe beam is refracted. The refraction of the beam shifts the power from one photo diode cell to the other, which produces a "difference" output voltage. In the experiments, the dual photo diode was placed a few cm in front of the image point, where it gave a sensitivity of ≈0.5 degrees per volt. Spurious differences in the two diodes due to differential absorption in the inhomogeneous plasma might be a concern. Such absorption is mainly due to inverse bremsstrahlung [7]. For the typical electron density of ≈1–5 × 10^{19} cm^{-3}, mean charge Z of 10 for neon, temperature of 100 eV, and optical path length of 0.5 mm in a 0.3 MA pinch, the absorption is estimated to be <1–5% at the 6000 Å laser wavelength. Indeed, the differential signal of the photodiodes cannot distinguish between absorption and deflection, but the sum signal of the photodiodes *does* monitor the absorption when compared with the reference laser intensity (i.e., the S-polarized component of the laser). Such absorption was checked in earlier experiments and was not detectable even at the 1% level. Absorption was therefore not considered further.

By using a visible light camera to image the pinch plasma region, the relative position of the laser beam to the pinch plasma was determined from the captured image. Fig. 3 shows the visible light image of the pinch plasma and the laser spot. The camera has a magnification of ≈10:1 and a spatial resolution of ≈10 μm. The diameter of the pinch plasma was about 0.5 mm. Since the pinch plasma radiation is much weaker than that of the laser radiation, the 1000× attenuation filter in front of the camera was removed. As a result, the laser spot is saturated. Instead of a ≈50 μm diameter spot, it appears to be much larger. Such images served to give the precise radial location of the laser for all the measurements.

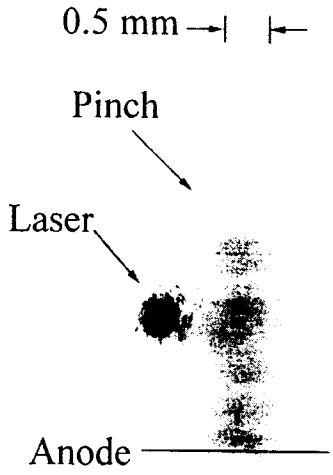

Fig. 3. Visible light image of the pinch plasma and the laser spot. Since the laser spot is saturated, it appears much larger than its true size of ≈50 μm diameter.

The experimental data from the single beam refraction and polarization rotation measurements are shown in Figs. 4–6. Fig. 4(a) shows a typical DPF current pulse and the corresponding neon K-shell X-ray signal. The peak current is about 0.3 MA with a rise time of ≈1.7 μs, measured by a Rogowski coil embedded in the base of the 9.5 cm long, 3.5 cm diameter anode. This current is measured outside the vacuum, upstream of the DPF electrodes. Small dB/dt sensors could be used to measure the current within the electrodes but tend to perturb the sheath dynamics so were not used for these experiments. The sudden drop of the current at pinch time is due to the large inductance increase of the imploding pinch. The X-ray emission occurs as a brief pulse of ≈10 ns duration coincident with the rapid dip seen in the current trace. The trace in the figure is a saturated p-i-n diode signal. The true pulse width of the K-shell X-ray radiation [11] measured with fast photoconducting diamond detectors is about 10 ns. The total neon K-shell radiation energy is about 15 J. The S-polarization component of the 3 ns laser pulse is superimposed on the X-ray signal so that the relative timing of the laser pulse to the pinch plasma is obtained.

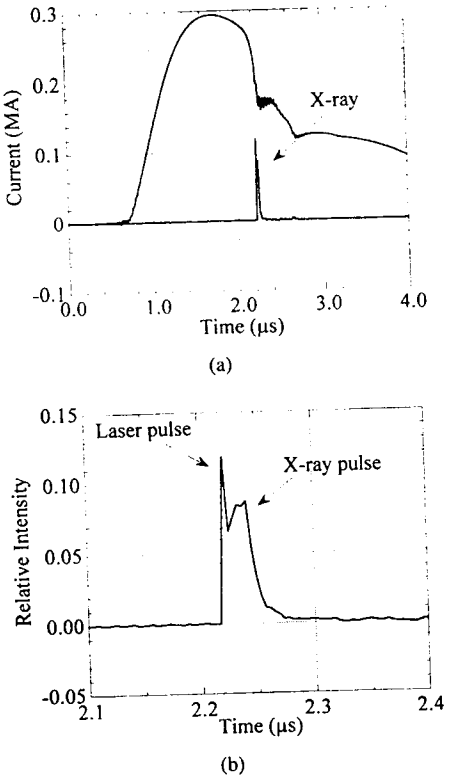

Fig. 4. (a) The current pulse (solid line) and the X-ray emission (dashed line) versus time; (b) the ≈3 ns laser pulse is shown superimposed on the X-ray signal on an expanded time scale. The total Ne K-shell soft X-ray output was ≈15 J with a FWHM pulse width of ≈10 ns. The delay time between the X-ray emission and the laser pulse is about 5 ns, taking the cable delay into account.

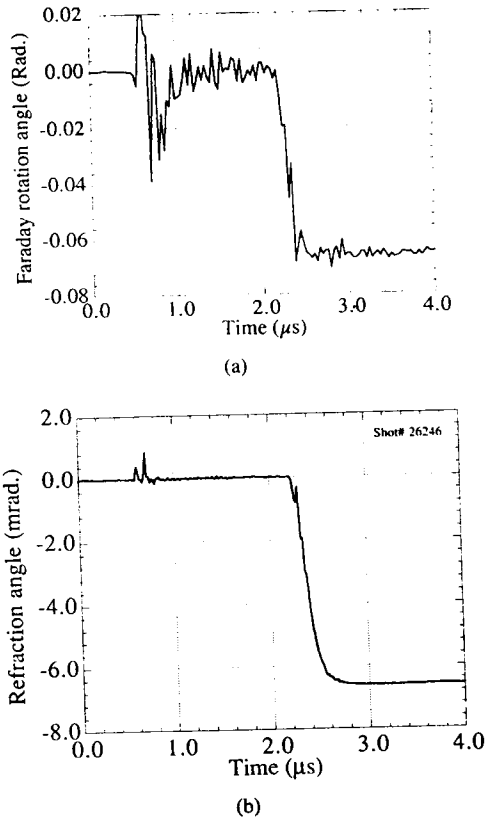

Fig. 5. (a)–(b) Measured Faraday rotation and deflection angles versus time. The noise spikes at $t \approx 0.6$ μs are due to the trigger noise of the discharge. The delay time is about 5 ns and the separation between the laser probe beam and the pinch axis was $y = 0.2$ mm. The measured Faraday rotation and refraction angles are ≈0.06 radians and 6 mrad, respectively.

Fig. 4(b) shows the Neon K-shell X-ray emission and probe laser beam signals on an expanded time scale. The relative position of the laser beam in the pinch plasma was obtained from the visible light image described earlier. The diameter of the pinch plasma was ≈0.5 mm measured from these images. Since the peak implosion current was only ≈0.3 MA, the Faraday rotation and beam refraction angles were not measurable during the axial run down and radial implosion phases. When the laser beam was closer to the final pinch plasma, Faraday rotation and refraction of the laser beam due to the interaction with the tight pinch plasma were observed as shown in Fig. 5.

Fig. 5(a) and (b) show the differential signals from the polarization analyzer (Faraday rotation) and the dual photo diodes (refraction), respectively. The laser pulse occurred about 3 ns prior to the pinch plasma as measured. Since the time response of the photo diodes was slower (≥50 ns) than the 3 ns laser pulse, the detectors were operated in a time integrated mode. The levels of these time integrated signals (which also improved the signal to noise ratios) gave Faraday rotation and refraction angles at a given laser delay time with respect to the pinch. Peak polarization rotation and beam refraction angles of ~0.06 and 0.006 radians were measured, respectively. If a longer pulse laser were used along with fast photo-diodes, then the temporal evolution of the density and magnetic field could have been measured on a single shot. Here we took advantage of the 4 Hz rep-rate of the DPF to gather time integrated data, but at several different delays of the probe laser relative to the pinch. The measurements were taken along two chords at positions of $y = +0.2$ and $y = -0.27$ mm, where the plus (or minus) sign of y means that the laser beam was on either side of the pinch axis. Data were obtained with various delay times between the laser and the pinch plasma.

Fig. 6(a) and (b) show the Faraday rotation and refraction angles as a function of these delay times at $y = 0.2$ mm. Observe that there is Faraday rotation or refraction only when the probe laser is coincident with the ≈10 ns interval of the dense pinch. For this 0.3 MA machine, the technique is not sensitive enough to measure the density and current when the current sheath is at larger radii. However, such data might be obtained in higher current machines. For a fixed y position, the maximum Faraday rotation and refraction angles should occur when the plasma radius is $0.83y$ and $1.25y$, respectively, as may be derived from (5) and (6). Therefore, during the collapse of the pinch plasma onto the z-axis, the peak of the refraction angle should occur slightly earlier than the peak of the Faraday rotation angle. The data of Fig. 6 do not show this clearly because the 3 ns laser pulse probably smeared this effect. The electron line density and the current are derived from the measured peak values of the refraction and polarization rotation angles. At a given distance y the refraction (or Faraday rotation) angle reaches its maximum when y/R is 0.83 (or

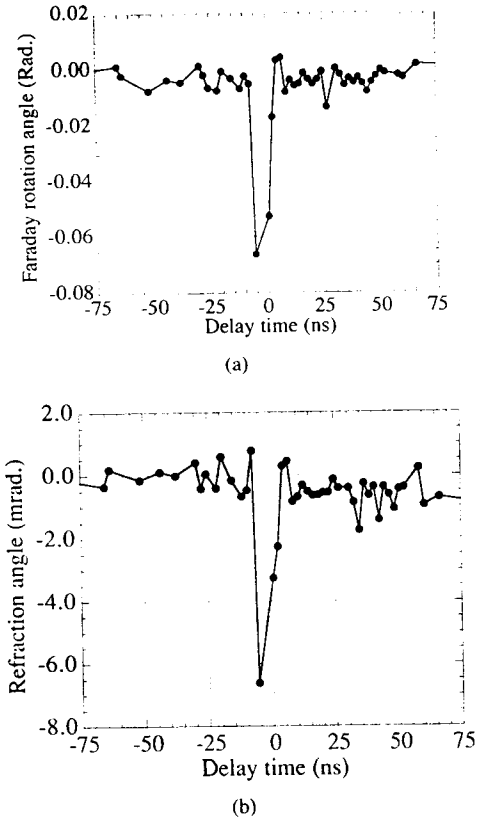

Fig. 6. (a)–(b): Faraday rotation angle and deflection angle versus delay time between the pinch and the laser pulse. The pinch axis is horizontal. The signals are negative when the probe beam is on the upper side of the pinch axis, i.e., at $y = 0.01$ cm from the pinch axis.

TABLE II
EXPERIMENT RESULTS OF BEAM DEFLECTION AND POLARIZATION MEASUREMENTS

Distance y (mm)	Maximum FR angle (rad.)	Maximum deflection angle (mrad.)	Electron density from the refraction angle (cm^{-3})	Current from the FR angle (MA)	Current from Rogowski coil (MA)
0.2	0.066	6.6	2.5×10^{19}	0.25±0.02	0.22
-0.27	0.044	5.1	3.5×10^{19}	0.21±0.02	0.22

1.25). From (5) and (6)

$$N\ (\mathrm{cm}^{-1}) = 1.9 \times 10^{22} y^2 \theta_r \tag{8}$$

and

$$I\ (\mathrm{MA}) = 0.025 \theta_f / \theta_r \tag{9}$$

where y/R of 0.83 and 1.25 are used in (8) and (9), respectively.

Table II shows the measured peak Faraday rotation and refraction angles and the corresponding deduced electron density and pinch current at two radial positions, when a pinch plasma radius of 0.25 mm was assumed for the density estimate. The measured central electron density and pinch current are 2.5 $\pm$ 0.5 $\times$ 10^{19} cm^{-3} and 0.25 $\pm$ 0.02 MA, respectively. The current measured by the upstream Rogowski coil located at the base of the anode (outside the vacuum) was 0.22 $\pm$ 0.01

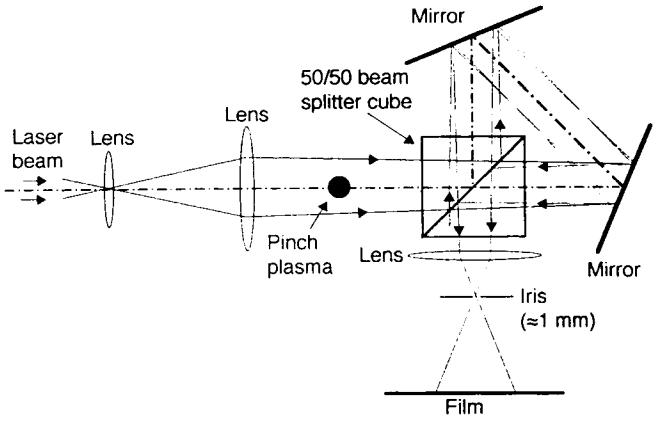

Fig. 7. Optical arrangement for the shearing interferograms. The magnification of the pinch plasma on the film is 1.6:1.

MA. The current derived from the Faraday rotation angle at the distance $y = 0.2$ mm is slightly higher than that from the Rogowski coil. The 0.2 mm distance is less than the typical pinch radius of 0.25 mm. Some of the current could flow at a larger radius ($\geq$0.2 mm), so (6) artificially enhances the "Faraday" current relative to the upstream Rogowski. To within the accuracy of the measurements, the agreement is encouraging. More accurate comparison requires modification of (6) to more accurately derive the Faraday current. At a distance of $y = 0.27$ mm, the density and "Faraday" current are 3.5±0.5 $\times$ 10^{19} cm^{-3} and 0.21±0.02 MA, respectively. Now the Faraday current agrees more closely with the upstream Rogowski (0.22 MA) as expected. These data suggest that the current is confined to the high density pinch. To our knowledge, these are the first such current measurements within one or two final radii of high current pinches.

B. Shearing Interferograms

For the shearing interferograms, the 10 μJ, 3 ns FWHM, 6000 Å wavelength laser beam was expanded to $\approx$20 mm diameter. After passing through the pinch plasma, the 20 mm diameter collimated laser beam was sheared by the shearing interferometer. This interferometer consists of two mirrors and a beam splitter cube as shown in Fig. 7. A camera was used to capture images on film with a magnification of 1.6:1. Polaroid type 55 positive/negative instant film was used to record shearing interferograms. For a good exposure of the film, the energy required is about 1 $\mu J/cm^{-2}$. Therefore, the laser output ($\sim$10 μJ) was sufficient to expose several square centimeters of film. Shearing perpendicular and parallel to the pinch axis were measured separately. With various delay times between the laser pulse and the pinch plasma, interferograms were taken and later digitized with a resolution of $\sim$10 line pairs/mm. From these interferograms, the dynamics of the implosion were measured and the implosion velocities obtained.

Fig. 8 shows a schematic drawing of the experimental arrangement. Without the plasma, a more or less uniform fringe pattern is expected, which serves as the reference fringe pattern. The inset in the figure shows such a pattern, measured when the pinch was not fired. The several dark semicircles at the bottom of the image are the shadows of a few of the

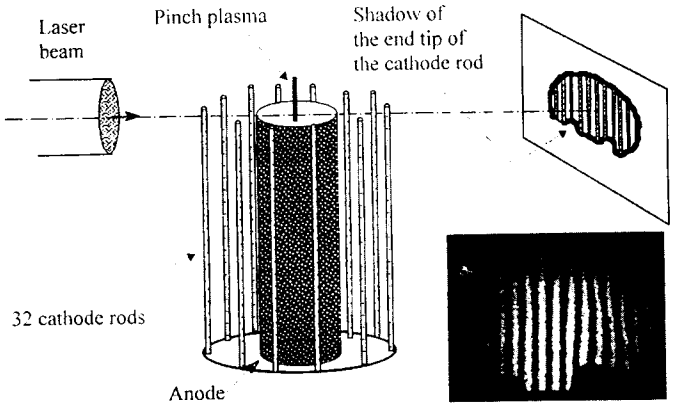

Fig. 8. Schematic drawing of the shearing interferogram images. The measured fringe pattern shown in the lower right corner was obtained without the DPF discharge and serves as a reference pattern for quantitative density measurements.

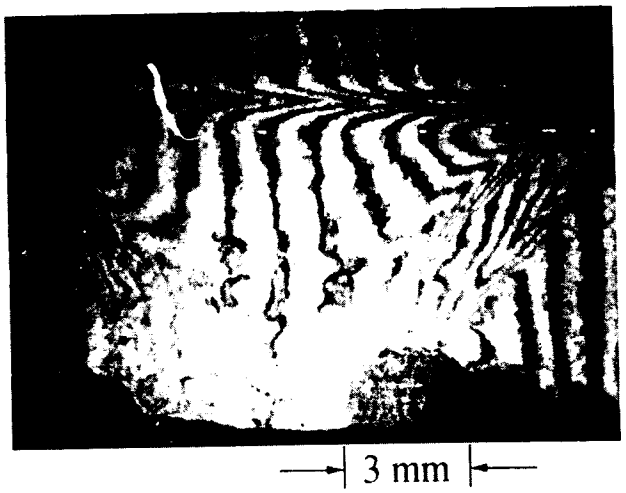

(a)

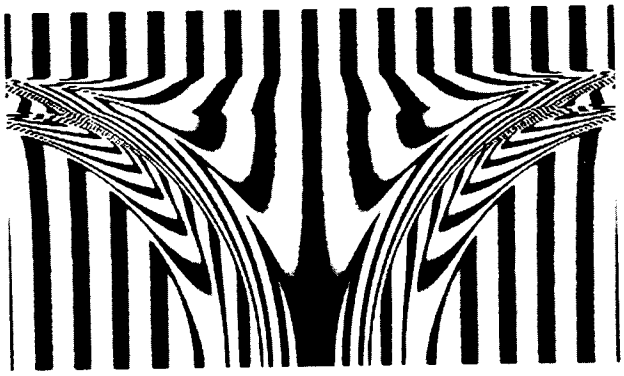

(b)

Fig. 9. (a) Shearing interferogram of the imploding current sheath at large radius, prior to assembly on axis as a dense pinch; (b) numerical simulation of the shearing interferogram of the imploding plasma (see text for details).

cathode rods' end tips. These fringes were produced by proper adjustment of the displacement of the sheared laser beams. A portion of the expanded laser beam was occulted by the anode and the end tips of the cathode rods.

Fig. 9(a) shows a shearing interferogram obtained when the laser beam was coincident with the imploding current sheath,

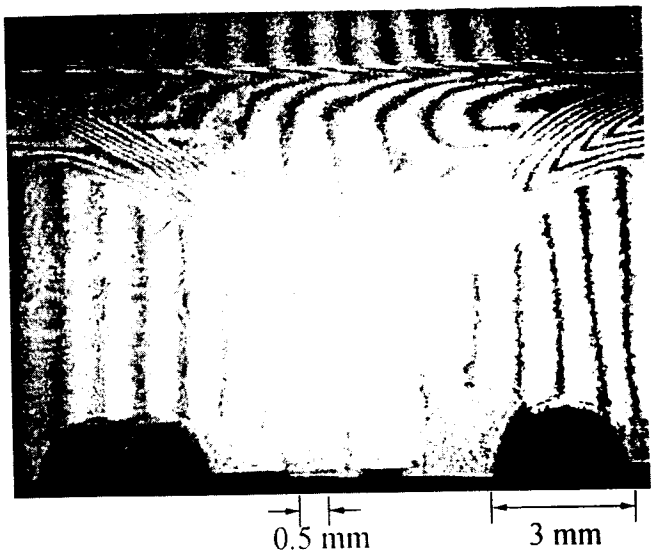

Fig. 10. Shearing interferogram of the current sheath after it has assembled on axis to form a tight pinch. Note that the fringes inside the pinch are smeared out by motion during the ≈3 ns laser pulse and also by strong density gradients.

but at a radius of ≈5 mm, well before the final pinch. In this arrangement, the shearing was 1.6 mm parallel to the z-axis as measured from the image. Unlike a typical cylindrical Z-pinch plasma, which is more or less uniform in the z-direction, the DPF plasma looks like a toroidal shell from the image. The nearly parallel vertical fringes on the axis of the pinch and in regions outside the thin current sheath represent the undisturbed wavefronts. Within the current sheath, each of these undisturbed fringes is observed to be heavily distorted before it emerges on the other side of the sheath as an undisturbed fringe. Figure 9(b) shows a numerical simulation of the shearing interferogram. For the simulation, a uniform toroidal shell of plasma was assumed, with a mean diameter of 15.8 mm and a 1.6 mm thickness. One wave of fringe shift requires a density in such a shell of 2.75×10^{18} cm^{-3}. Since the measured image showed ≈1.2 waves, the density was taken to be 3.3×10^{18} cm^{-3} in the thin shell. Comparing Fig. 9(b) to (a), the simulation of some portion of the shearing fringe pattern matches well with the observation. The analysis would be more refined if the diffraction of the plasma and variation of the electron density in the shell were included in the simulation, or by constructing a sophisticated code, the electron density map could be derived from these fringe shift patterns. As a rough estimate, if one assumes that when the toroidal shell collapses on itself, the current sheath is compressed by a factor of 6.4 from 1.6 mm to 0.25 mm radius, then the density is expected to increase by a factor of 40 from 3.3×10^{18} cm^{-3} up to $\approx 1.3 \times 10^{20}$ cm^{-3}. This estimate is higher than that from the refraction measurements described earlier ($\approx 3.5 \times 10^{19}$ cm^{-3}) and with other spectroscopic estimates [13], but is consistent with the fact that the pinch collapse in DPF's is always accompanied by mass loss axially and that the refraction data were obtained at a radius that did not include the core of the pinch.

Fig. 10 shows a shearing interferogram obtained when the laser beam captured the imploding current sheath just as it

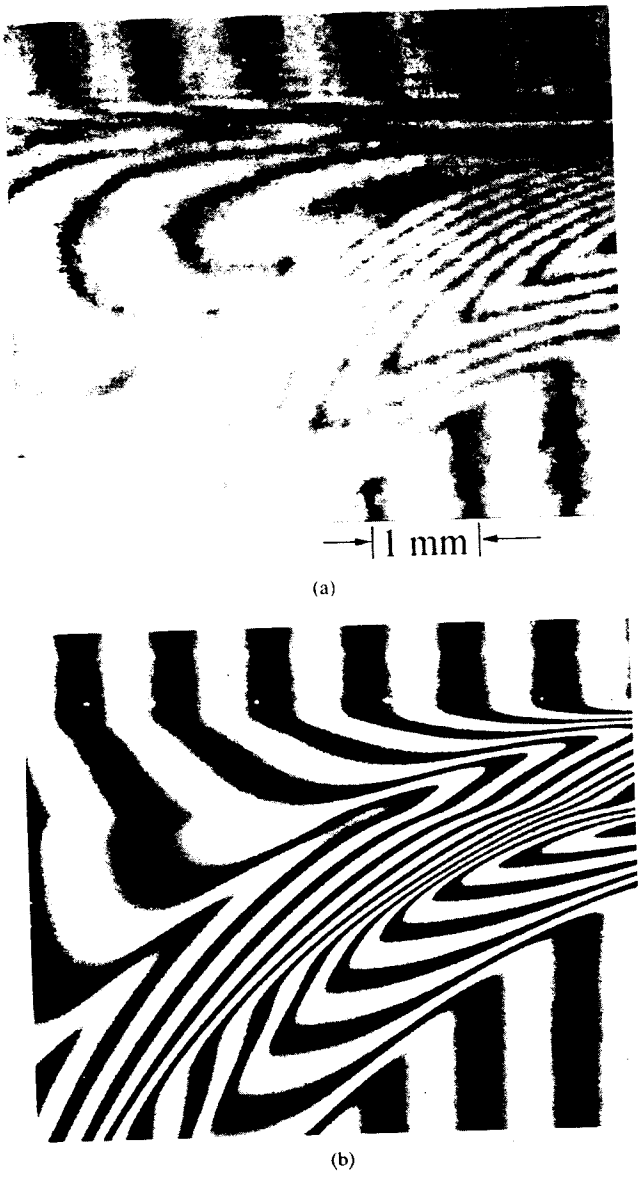

Fig. 11. (a) Expanded view of a portion of the shearing interferogram of Fig. 10; (b) numerical simulation of the shearing interferogram assuming that the current sheath is a uniform, toroidal shell (see text for details).

pinched on the axis. The pinch occurs when the major radius of the torus equals the minor radius. The length of the pinch plasma is an increasing function of time as the toroidal shell collapses on to the axis. Clearly defined fringes are observed only in the region of the current sheet that is outside the Z-pinch. The Z-pinch itself looks more like a double shadowgram than a fringe pattern. This is due to the refraction of the laser beam out of the shearing instrument and/or the movement of the pinch plasma during the 3 ns laser pulse, which could smear the fringes. Notice the fringes in the image were about $\sim$10 lines/mm. Typical plasma radial implosion velocities were $\sim 10^7$ cm/s, (see discussions after the next paragraph) and the diameter of the pinch plasma was $\approx$0.5 mm. During the 3 ns laser pulse, the pinch plasma moved about 0.3 mm. Any fringes in the pinch plasma could be smeared out due to this plasma motion.

Fig. 11(a) and (b) shows an enlargement of the interferogram of Fig. 10 and the simulated shearing interferogram, respectively. From the laser beam refraction measurements, an electron density of 3×10^{19} cm^{-3} and electron line density of $\sim 6 \times 10^{16}$ cm^{-1} were obtained. The electron density of 4.4×10^{18} cm^{-3} in the shell used to simulate the interferogram is less than that in the pinch. but gradients and plasma diffraction have not been included. Nevertheless, the similarity between Fig. 11(a) and (b) gives confidence that a more sophisticated numerical procedure [14], [15] can provide detailed density maps from such images.

Fig. 12 shows the shearing interferograms for a sequence of delay times between the laser and the pinch. In this case, shearing was set *transverse* to the pinch axis, so no density data were expected. The purpose of these images was to deduce radial and axial velocities, as shown below. The toroidal shell shaped current sheath not only implodes toward the z-axis, but also propagates along the z-axis. Fringes of the current sheath (due to electrons) along and toward the pinch axis were observed. From these shearing interferograms, it is estimated that the diameter of the pinch are about 0.5 mm.

The pinch plasma radius and the current sheath motion along the pinch axis as a function of time are shown in Fig. 13(a) and (b), respectively. The typical radial implosion velocity is about 2×10^7 cm/s. This implies that the kinetic energy of the neon ions is on the order of that required to reach the K-shell ionization stage. The current sheath propagates along the z-axis with a velocity of $\sim 5 \times 10^6$ cm/s. As shown in Fig. 12(f)–(i), the plasma stagnated on the z-axis within a duration of $\sim$10 ns. This is close to the measured 10 ns X-ray pulse width (FWHM). Due to the toroid shaped current sheath (the z-variation of the plasma), zippering effects of the pinch plasma are observed. Zippering refers to a nonuniform assembly of the pinch on axis, wherein the pinch first forms in a local region close to either electrode and gradually elongates as other regions become dense and hot. Zippering is a problem for high current Z-pinches because it reduces the pinch density and smears out the X-ray pulse, reducing the peak X-ray power output of the simulator. This shearing interferogram technique appears to provide a simple yet powerful measure of zippering. The length of the pinch plasma increased by 2 mm in $\sim$8 ns, while the front of the current sheath was stalled at $z = 6.8$ mm [Figs. 12(i)–(l)].

IV. Conclusion

In summary, electron density and implosion current in a dense DPF plasma were measured using laser beam refraction and polarization methods. Shearing interferograms of a Z-pinch plasma were also obtained. These measurements provided the pinch electron density, the current flowing in the plasma, and the dynamics of the DPF implosion. The measured electron density in the pinch plasma was about 3×10^{19} cm^{-3}. It was found that most of the 0.3 MA implosion current flows within the final pinch plasma. Images of the toroidal shell shaped current sheath were obtained.

These experiments have produced results that strongly motivate similar measurements on higher current drivers, such as Double Eagle, Syrinx, Saturn, Decade-Quad, and PBFA Z. To conduct similar experiments on higher current simulators, several key issues should be resolved. The probe laser energy

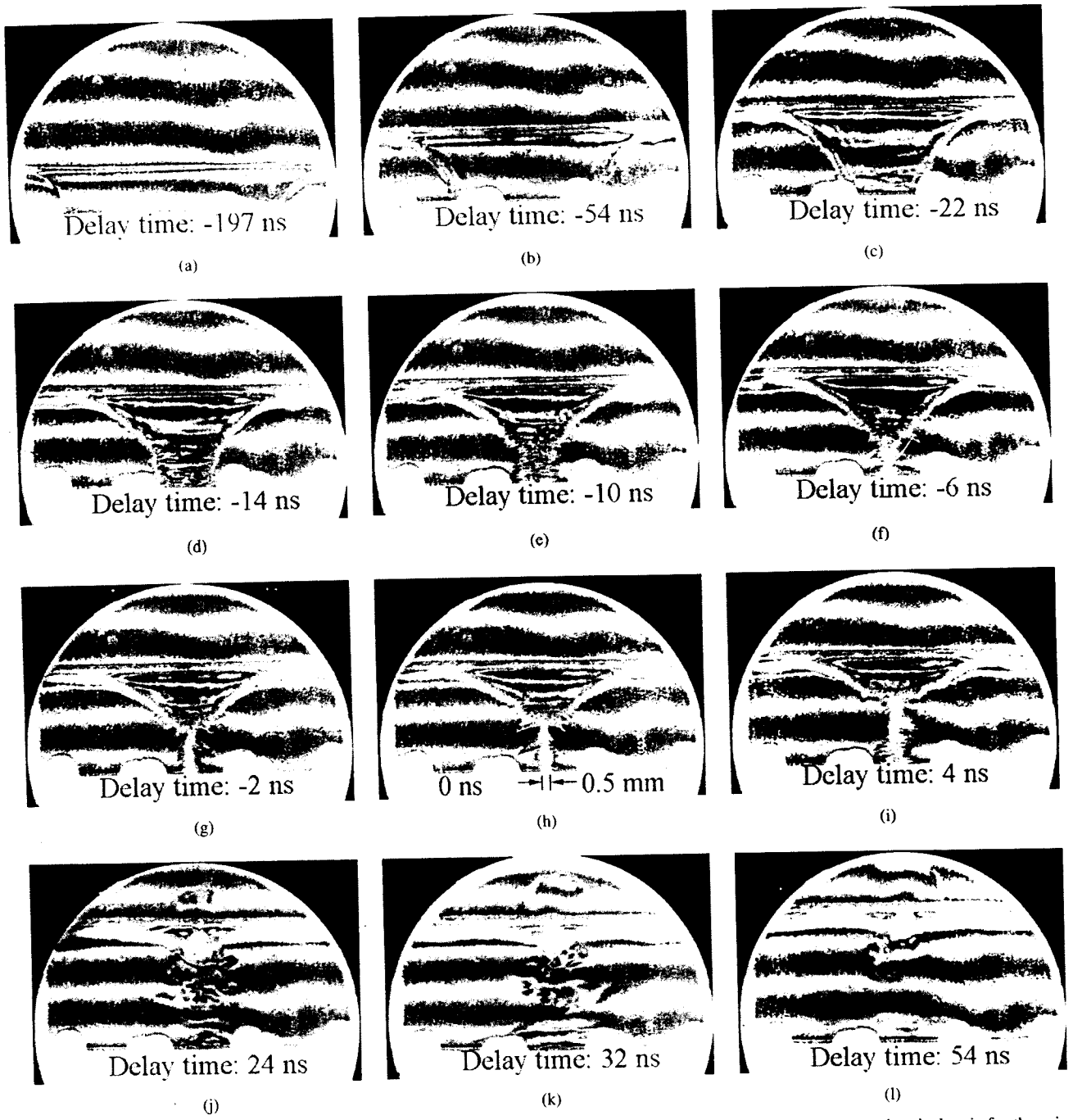

Fig. 12. A sequence of shearing interferograms as a function of laser delay time. Note that the shearing was *transverse* to the pinch axis for these images, so no density information is obtained. The purpose of these images was to measure the radial and axial velocities of the imploding current sheath.

used in our experiment was only ~10 μJ/3 ns and yet gave good signal/background, with only a crude bandpass filter and no spatial filtering. With better filters, a 100 mJ/100 ns laser should be adequate to probe at least the outer regions of 3–20 MA pinches with high accuracy. In the experiments described here, the time resolved refraction and Faraday rotation angle measurements required hundreds of shots because a single short pulse (≈3 ns) laser was used. It is too costly to use a single short pulse laser probe on high current Z-pinches because too many shots are required. However, if one used a long pulse width laser (say 200 ns wide) and fast response (≈1 ns) photo detectors, these angles can be measured with continuous and high time resolution on a single high current simulator shot. Use of a multichannel laser probe through several chords in the pinch plasma simultaneously will make obtaining the electron density and current profiles even more practical. For shearing interferometry, a short pulse laser (~10 mJ/50 ps) is required to "freeze" the plasma motion and avoid smearing of fringes. A combination of the laser beam refraction and rotation angle measurements along several chords, along with the 2-D shearing interferometry at several delay times (using two very *different* probe lasers) will enable us to obtain time resolved density and current profiles of imploded plasmas. Note that for high current machines, the

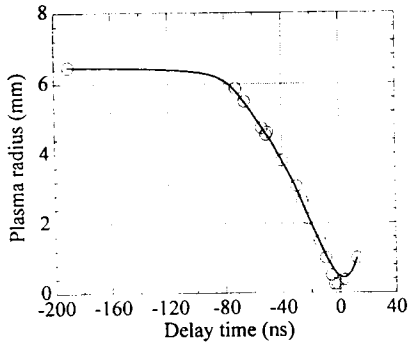

Fig. 13. (a)–(b): Radial and axial positions of the current sheath as a function of time, as deduced from the images of Fig. 12.

core of the pinch plasma may be too dense to be measured even with a UV wavelength laser. However, a corona is usually present outside the core. The electron density is much lower in this corona but the self magnetic field has not decreased significantly, rolling off as $1/r$. The beam refraction and polarization angles near the corona can be measured at a radius comparable to the pinch plasma size. Since today's high current Z-pinches allow current measurements only at radii of ≥ 10 times the pinch radius, even the coronal measurements proposed here would be a breakthrough.

ACKNOWLEDGMENT

The authors would like to express their appreciation to Dr. G. Rondeau for assistance with the experiments and for many helpful discussions.

REFERENCES

[1] S. Czekaj, A. Kasperczuk, R. Mikaszewski, M. Paduch, T. Pisarczyk, and Z. Wcreszczynski, "Diagnostic method for the magnetic field measurement in the plasma focus device," *Plasma Phys. Control Fusion*, vol. 31, pp. 587–594, Feb. 1989.

[2] D. Jackson, N. M. Amer, A. C. Boccara, and D. Fournier, "Photothermal deflection spectroscopy and detection," *Appl. Opt.*, vol. 20, pp. 1333–1344, Oct. 1981.

[3] V. Greco, G. Molesini, and F. Quercioli, "Accurate polarization interferometer," *Rev. Sci. Instrum.*, vol. 66, no. 7, pp. 3729–3734, 1995.

[4] A. J. H. Donne, "High spatial resolution interferometry and polarimetry in hot plasmas," *Rev. Sci. Instrum.*, vol. 66, no. 6, pp. 3407–3423, 1995.

[5] M. Murty, "Lateral shearing interferometers," in *Optical Shop Testing*, D. Malacara, Ed. New York: Wiley, 1978.

[6] P. Hariharan and D. Sen, "Cyclic shearing interferometer," *Rev. Sci. Instrum.*, vol. 37, pp. 372–382, Apr. 1960.

[7] I. H. Hutchinson, *Principles of Plasma Diagnostics*. Cambridge, U.K.: Cambridge Univ. Press, 1987.

[8] W. H. Bennett, "Magnetical self-focussing streams," *Phys. Rev.*, vol. 45, no. 2, pp. 890–895, 1934.

[9] G. Decker, R. Deutsch, W. Kies, and R. Rybach, "Plasma layer of fast focus discharges—Schlieren pictures experimentally taken and computer simulated," *Plasma Phys.*, vol. 27, pp. 609–619, Oct. 1985.

[10] R. Aliaga, P. Choi, and H. Chuaqui, "Circular encoding in large area multi-exposure holography," presented at *SPIE-Int. Soc. Opt. Eng. 1358, 19th Int. Congr. High-Speed Photography Photonics*, Cambridge, U.K., 1990.

[11] R. R. Prasad, M. Krishnan, J. Mangano, P. A. Greene, and N. Qi, "Neon dense plasma focus point X-ray source for ≤ 25 μm lithography," *Proc. SPIE-Int. Soc. Opt. Eng.*, vol. 2194, pp. 120–128, 1994.

[12] M. Mathuthu, T. G. Zengeni, and A. V. Gholap, "The three-phase theory for plasma focus devices," *IEEE Trans. Plasma Sci.*, vol. 25, no. 6, pp. 1382–1388, 1997.

[13] P. Burkhalter, G. Mehlman, D. A. Newman, M. Krishnan, and P. R. Prasad, "Quantitative X-ray emission from a DPF device," *Rev. Sci. Instrum.*, vol. 63, pp. 5052–5055, Mar. 1992.

[14] S. Waldner, "Removing the image doubling in shearography by reconstruction of the displacement field," *Opt. Comm.*, vol. 127, no. 12, pp. 117–126, 1996.

[15] H. A. Aebischer and P. Rechsteiner, "Theoretical prediction of the effect of shear distortion in the michelson interferometer," *Pure Appl. Opt.*, vol. 6, no. 2, pp. 303–315, 1997.

Niansheng Qi (M'97), for a photograph and biography, see p. 1061 of the June 1998 issue of this TRANSACTIONS.

Stephen F. Fulghum received the B.S. degree in physics from Washington and Lee University, Lexington, VA, in 1969. He received the Ph.D. in physics from the Massachusetts Institute of Technology, Cambridge, in 1980 for research on the relaxation kinetics of the XeF molecule.

From 1971 to 1973, he served as a Lieutenant in the Advanced Concepts Office of the United States Army Strategic Communications Command. He began his work on interferometry by measuring transient refractive index effects in e-beam-pumped excimer lasers at the Avco Everett Research Laboratory, Everett, MA, in the 1980's. In 1987 he joined Science Research Laboratory (SRL), Somerville, MA, to develop ultra-sensitive interferometric calorimeters to measure atmospheric absorption at 1.06 micrometers. At SRL he has developed two-color laser interferometers for the measurement of electron densities and neutral gas densities in plasma erosion opening switches and Sagnac interferometers for the measurement of 193 nm absorption in fused silica.

Rahul R. Prasad (M'88) was born in New Delhi, India, in 1961. He received the B.Sc. degree in physics from St. Stephen's College, New Delhi, India, in 1982, and the Ph.D. degree in applied physics from Yale University, New Haven, CT, in 1987.

After a brief stint in the Mechanical Engineering Department of Yale University where he studied fractal behavior in turbulent fluid flows (winning an APS Flow Visualization award), he joined Physics International Company in California to work on megampere pulsed power driven Z-pinches and X-ray lasers. From 1991–1994, he was with the Science Research Laboratory, Alameda, CA, working on X-ray sources for lithography, vacuum arc centrifuges for isotope enrichment, and dense Z-pinches. He co-founded Alameda Applied Sciences Corporation in 1994, is Principal Scientist, and works on high voltage, fast diamond switches, diamond radiation detectors, ion sources, and fiber optic sensors.

Mahadevan Krishnan (M'90), for a photograph and biography, see p. 1061 of the June 1998 issue of this TRANSACTIONS.